Available online at www.sciencedirect.com
SCIENCE DIRECT®
Biochemical and Biophysical Research Communications 325 (2004) 10–17
BBRC
www.elsevier.com/locate/ybbrc

Interaction of shikimic acid with shikimate kinase

José Henrique Pereira[a], Jaim Simões de Oliveira[b], Fernanda [illegible]duri[a,c], Marcio Vinicius Bertacine Dias[a], Mário Sérgio Palma[c,d], Luiz Augusto Basso[b], Walter Filgueira de Azevedo Jr.[a,d,*], Diógenes Santiago [illegible]ntos[e,*]

[a] Department of Physics, UNESP, São José do Rio Preto, SP 15[illegible]000, Brazil
[b] Rede Brasileira de Pesquisa em Tuberculose Grupo de Microbiologia Molecular e Funcional, Dep[illegible]ia Molecular e Biotecnologia, UFRGS, Porto Alegre, RS 91501-970, Bra[illegible]
[c] Center for Applied Toxinology, Institute Butantan, São Pa[illegible] SP 05503[illegible]azil
[d] Laboratory of Structural Biology and Zoochemistry, CEIS/Department of Biology, Insti[illegible]sciences, U[illegible]ESP, Rio Claro, SP 13506-900, Brazil
[e] Centro de Pesquisa e Desenvolvimento em Biologia Molecular e Funcional, Pontifícia Universi[illegible] Católica do Rio Grande do Sul, Porto Alegre, RS 90619-900, Brazil

Received 24 Septem[illegible] 2004
Available online 19 O[illegible]ber 2004

RETRACTED

Abstract

The crystal structure of shikimate kinase from *M[illegible]cterium tuberculosis* (MtSK) complexed with MgADP and shikimic acid (shikimate) has been determined at 2.3 Å resoluti[illegible], cle[illegible]y revea[illegible]g the amino acid residues involved in shikimate binding. In MtSK, the Glu61 strictly conserved in SK form[illegible] hydr[illegible]nd and salt-bridge with Arg58 and assists in positioning the guanidinium group of Arg58 for shikimate bindi[illegible]. T[illegible]boxyl group of shikimate interacts with Arg58, Gly81, and Arg136, and hydroxyl groups with Asp34 and Gly80. [illegible] crystal[illegible]ucture of MtSK–MgADP–shikimate will provide crucial information for elucidation of the mechanism of SK-cat[illegible] reaction a[illegible] for the development of a new generation of drugs against tuberculosis.
© 2004 Elsevier Inc. All rights reserved.

Keywords: Drug design; *Mycobacte[illegible]m tube[illegible]losis*; Shikimate kinase; Structure; Shikimic acid

The shikimate ki[illegible]se (S[illegible]; EC 2[illegible].1.71), the fifth enzyme of the pathw[illegible] cat[illegible] specific phosphorylation of the 3-hydroxy[illegible]oup of shikimic acid using ATP as a co-substrate. In *Esc[illegible]ichia coli*, the SK reaction is catalyzed by two isoforms SK I encoded by the *aroK* gene [1] and SK II encoded by the *aroL* gene [2]. The major difference between the isoenzymes is their K_m for shikimate, 0.2 mM for the SK II and 20 mM for the SK I enzyme [3]. The SK II isoform appears to play a dominant role in the shikimate pathway, its expression is controlled by the *tyr*R regulator, and it is repressed by tyrosine and tryptophan [4,5]. The physiological role of SK I in *E. coli* is not clear. Since mutations in SK I are associated with sensitivity to the antibiotic mecillinam [6] it has been suggested that SK I may have an alternative biological role in which it phosphorylates shikimate only fortuitously [3]. Contrary to the presence of isoenzymes in *E. coli*, complete genome sequences of a number of bacteria, for example, *Haemophilus influenzae* and *Mycobacterium tuberculosis*, have revealed the presence of only one SK-coding gene. Most of these SKs appear to be encoded by *aroK* rather than *aroL* because their amino acid sequences have higher degree of identity with *E. coli* SK I. The kinetic parameters for *aroK*-encoded MtSK are more similar to those of *aroL*-encoded *E. coli* SK II than to those of *aroK*-encoded *E. coli* SK I. The MtSK K_m value (0.41 mM) for shikimate suggests that

* Corresponding authors.
E-mail addresses: walterfa@df.ibilce.unesp.br (W.F. de Azevedo Jr.), diogenes@pucrs.br (D.S. Santos).

0006-291X/$ - see front matter © 2004 Elsevier Inc. All rights reserved.
doi:10.1016/j.bbrc.2004.09.217

not all *aroK*-encoded SKs have high K_m values for shikimate [7].

The three crystal structures of SK from *Erwinia chrysanthemi* (EcSK) [8,9], which is encoded by *aroL*, show that SK belongs to the same structural family of nucleoside monophosphate (NMP) kinases for which structures are known for adenylate kinase (AK) [10,11], guanylate kinase [12], uridylate kinase [13], and thymidine kinase [14]. The NMP kinases are composed of three domains: CORE, LID, and NMP-binding (NMPB) domains [15]. A characteristic feature of the NMP kinases is that they undergo large conformational changes during catalysis, for which AK is the most extensively studied [15]. There are two flexible regions of the structures that are responsible for movement: one is the NMP-binding site which is formed by a series helices between strands 2 and 3 of parallel β-sheet and the other is the LID domain, a region of varied size and structure following the fourth β-strand of the sheet [16,17,28]. In SK, the shikimate-binding (SB) domain corresponds to the NMPB domain of NMP kinases.

Three functional motifs of nucleotide-binding enzymes are recognizable in MtSK, including a Walker A-motif, a Walker B-motif, and an adenine-binding loop. The Walker A-motif is located between the first β-strand (β1) and first α-helix (α1), containing the GXXXXGKT/S conserved sequence [18], where X represents any residue. This motif forms the phosphate-binding loop (P-loop), a giant anion hole which accommodates the β-phosphate of the ADP by creating hydrogen bonds from several backbone amides [19]. In addition to the Walker A-motif, a second conserved sequence ZZDXXG called Walker B-motif [18] is observed, where Z represents a hydrophobic residue. An Asp-Ser replacement exists in MtSK. More recently, however, sequence and structural comparisons for all P-loop-fold proteins classified shikimate kinase in the DxD group of enzymes [20], which has a conserved DxD motif in strand 2. The Walker B motif consensus in shikimate kinases is ZZZTGGG and the second glycine (Gly80 in MtSK) has been implicated in hydrogen bonding to the γ-phosphate of ATP. The Walker B-motif provides a bond for the octahedral coordination of a Mg^{2+} cation, which, in turn, is coordinated to the β- and γ-phosphate groups of nucleoside triphosphates [18]. The adenine-binding loop motif may be described as a sequence stretch of I/VDXXX(X)XP [7]. This motif forms a loop that wraps around the adenine moiety of ATP, connecting the β5-strand with the C-terminal α8-helix. The present crystal structure of MtSK–shikimate–MgADP will provide crucial information for the design of non-promiscuous SK inhibitors that target both the shikimate- and ATP-binding pockets or uniquely, the shikimate-binding site.

Materials and methods

Crystallization. The MtSK was concentrated and dialyzed against 50 mM Na Hepes buffer, pH 7.5, containing 0.5 M NaCl and 5.0 mM $MgCl_2$. This protein solution was mixed with 13.0 mM shikimate and 13.0 mM ADP, and centrifuged prior to crystallization. The protein concentration was about 17.0 mg mL^{-1}. The crystals were obtained by the hanging-drop vapor-diffusion method. The well solution contained 0.1 M Na Hepes buffer, pH 7.5, 10% 2-propanol, and 35% PEG 3350, and the drop was a mixture of 1.0 μL well solution and 1.5 μL of the protein solution.

Data collection and processing. The set of MtSK–shikimate was collected at a wavelength of 1.431 Å using the Synchrotron Radiation Source (Station PCr, LNLS, Campinas-Brazil) [21] and a CCD detector (MARCCD). The cryoprotectant contained 15% glycerol, 12% PEG 3350, and 3% propanol. The crystal was flash-frozen at 104 K under cold nitrogen stream generated and maintained with an Oxford Cryosystem. The oscillation range used was 1.0°, crystal to detector distance was 90 mm and the exposure time was 50 s. The data set containing 166 frames was collected and processed to 2.3 Å resolution using the program MOSFLM [22] and scaled with SCALA [23].

Molecular replacement and crystallographic refinement. The crystal structure of the MtSK–MgADP–shikimate was determined by standard molecular replacement methods using the program AMoRe [24], using as search model the structure of MtSK–MgADP (PDB access code 1L4Y) [7]. After translation function computation the correlation was 65% and the R_{factor} 38.3%. The highest magnitude of correlation coefficient function was obtained for the Euler angles $\alpha = 54.85°$, $\beta = 85.32°$, and $\gamma = 91.90°$. The fractional coordinates are $T_x = 0.7336$, $T_y = 0.5326$, and $T_z = 0.2768$. The atomic positions obtained from molecular replacement were used to initiate the crystallographic refinement. Structure refinement was performed using X-PLOR [25]. In the following rigid-body refinement, the R_{factor} decreased from 38.3% to 35.8%. Further refinement continued with simulated annealing using the slow-cooling protocol, followed by alternate cycles of positional refinement and manual rebuilding using XtalView [26]. Finally, the positions of waters, MgADP, and shikimate were checked and corrected in $F_{obs} - F_{calc}$ maps. The final model has an R_{factor} of 20.7% and an R_{free} of 28.7%.

Root-mean-square deviation differences from ideal geometries for bond lengths, angles, and dihedrals were calculated with X-PLOR [25]. The overall stereochemical quality of the final model for MtSK–MgADP–shikimate was assessed by the program PROCHECK [27]. Atomic models were superposed using the program LSQKAB from CCP4 [23]. The molecular surface areas have been calculated using the program Swiss-PDBViewer v3.7 (www.expasy.org/spdbv), probe radius of 1.4 Å, and a fixed radius for all atoms.

Results and discussion

The crystals of MtSK–MgADP–shikimate were grown in the presence of 5.0 mM $MgCl_2$, 13.0 mM ADP, and 13.0 mM shikimate. The data set of MtSK–MgADP–shikimate was collected at 2.3 Å (Table 1) using the Synchrotron Radiation Source [21], and the structure was solved by molecular replacement. There is one molecule of MtSK–MgADP–shikimate in the asymmetric unit, containing residues 2–166, Mg^{2+}, ADP, shikimate, two Cl^- ions, and 144 water molecules. Therefore, the enzyme crystallized as an MtSK–MgADP–shikimate dead-end ternary complex. The N-terminal methionine residue is not observed and the

RETRACTED

Table 1
Summary of data collection statistics for MtSK–shikimate

Unit cell (Å)	$a = b = 62.91$, $c = 90.92$
Space group	$P3_221$
Number of measurements with $I > 2\sigma(I)$	34,274
Number of independent reflections	9563
Completeness in the range from 29.74 to 2.30 Å (%)	98.7
R_{sym}[a] (%)	3.0
Highest resolution shell (Å)	2.41–2.30
Completeness in the highest resolution shell (%)	98.7
R_{sym}[a] in the highest resolution shell (%)	7.20
R_{sym}[a] (for all data) (%)	3.1
Wilson B value	40.06

[a] $R_{sym} = 100 \sum|I(h) - \langle I(h)\rangle|/\sum I(h)$ with $I(h)$, observed intensity and $\langle I(h)\rangle$, mean intensity of reflection h overall measurement of $I(h)$.

10 C-terminal residues (NQIIHMLESN) are disordered. Details of refinement and final model statistics are presented in Table 2. Analysis of the Ramachandran diagram ϕ–ψ plot shows that 93.4% of non-glycine residues lie in the most favored regions and there are no residues in the disallowed region. The average B factor for main chain atoms is 34.64 Å^2, whereas that for side-chain atoms is 35.68 Å^2 (Table 2). In order to accurately determine the position of shikimate binding in the active site of MtSK, larger final concentrations of ADP and shikimate in the drop (8 mM) than those used by Gu et al. [7] are used to obtain the crystals (4 mM). The average B factor value of 26.15 Å^2 obtained for shikimate indicates a higher order and occupancy of this substrate in the present structure than in other SKs previously solved, where either shikimate was not complexed or its electron density was too poor to accurately locate this substrate (Table 2) [7,8].

Table 2
Summary of refinement statistics for MtSK–MgADP–shikimate

Resolution range (Å)	[illegible]
Data used for refinement	[illegible]
Number of residues	[illegible]
Number of water oxygen atoms	144
Number of ADP molecules	1
Number of metal ions (Mg^{2+})	1
Number of Cl^-	2
Number of shikimate molecules	1
Final R_{factor}[a] (%)	20.7
R_{factor}[a] (%) (for all data)	24.6
Final R_{free}[b] (%)	28.7
R_{free}[a] (%) (for all data)	30.3
B factors[c] (Å^2)	
Main chain	34.64
Side chains	35.68
Waters	39.63
ADP	21.81
Mg^{2+}	34.70
Cl^-	37.65
Shikimate	26.15
Observed rmsd from ideal geometry	
Bond lengths (Å)	0.017
Bond angles (°)	1.905
Dihedrals (°)	22.125
Ramachandran plot (%)	
Most favored Φ/Ψ angles	93.4
Disallowed Φ/Ψ angles	0

[a] $R_{factor} = 100 \times \sum|F_{obs} - F_{calc}|/\sum(F_{obs})$, the sums being taken overall reflections with $F/\sigma(F) > 2$ cutoff.

[b] $R_{free} = R_{factor}$ for 10% of the data, which were not included during crystallographic refinement.

[c] B values = average B values for all non-hydrogen atoms.

SK displays an α/β fold and consists of five central parallel β-sheets, flanked by α-helices. As pointed out above, a characteristic feature of SKs is that they undergo large conformational changes during catalysis. There are two flexible regions of the structures that are responsible for movement: SB and LID domains (Fig. 1), which in MtSK correspond to residues 33–61 and 112–124, respectively.

Shikimate-binding

The shikimate-binding domain, which follows strand β1, consists of the helices α2, α3, and N-terminal region of helix α4 (residues 33–61). A peak of more than 3σ in the $F_{obs} - F_{calc}$ difference Fourier map clearly indicates the position of bound shikimate in the electron density (Fig. 2).

The chemical structure of shikimic acid ([3R-(3α,4α,5β)]3,4,5-trihydroxy-1-cyclohexene-1-carboxylic acid) is shown in Fig. 3. The guanidinium group of Arg58 and Arg136, and the NH-backbone group of Gly81 interact with the carboxyl group of shikimate. The 3-hydroxyl group of shikimate forms hydrogen bonds with carboxyl group of Asp34, main chain NH group of Gly80, and a water molecule. This water molecule, in turn, mediates interactions with side-chains of SB residues Arg58 and Glu61; Walker-B residues Gly79, Gly80, and Gly81; and Ala82. The 2-hydroxyl group of shikimate hydrogen bonds to Asp34 side-chain. The distances of direct and water-mediated hydrogen bonds of shikimate binding in MtSK are shown in Table 3.

The residue Glu61 is conserved in both *aroK*- and *aroL*-encoded shikimate kinase enzymes and has been implicated in shikimate binding [7,8,29]. Krell et al. [8] proposed that Glu61 is suitably positioned to bind the 5-hydroxyl group of shikimate in EcSK. However, the amino acid residues comprising the shikimate binding domain were not clearly demonstrated because the electron density was not sufficient to position the shikimate molecule in the structure. In our structure, the Glu61 side-chain forms a water-mediated interaction with the 3-hydroxyl group of shikimate. In addition, the Glu61 forms a hydrogen bond and a salt-bridge with the conserved Arg58 and assists in positioning the guanidinium group of Arg58 for substrate binding through interactions with the carboxylate group of shikimate. The OE2 atom of Glu61 makes a hydrogen bond with the

RETRACTED

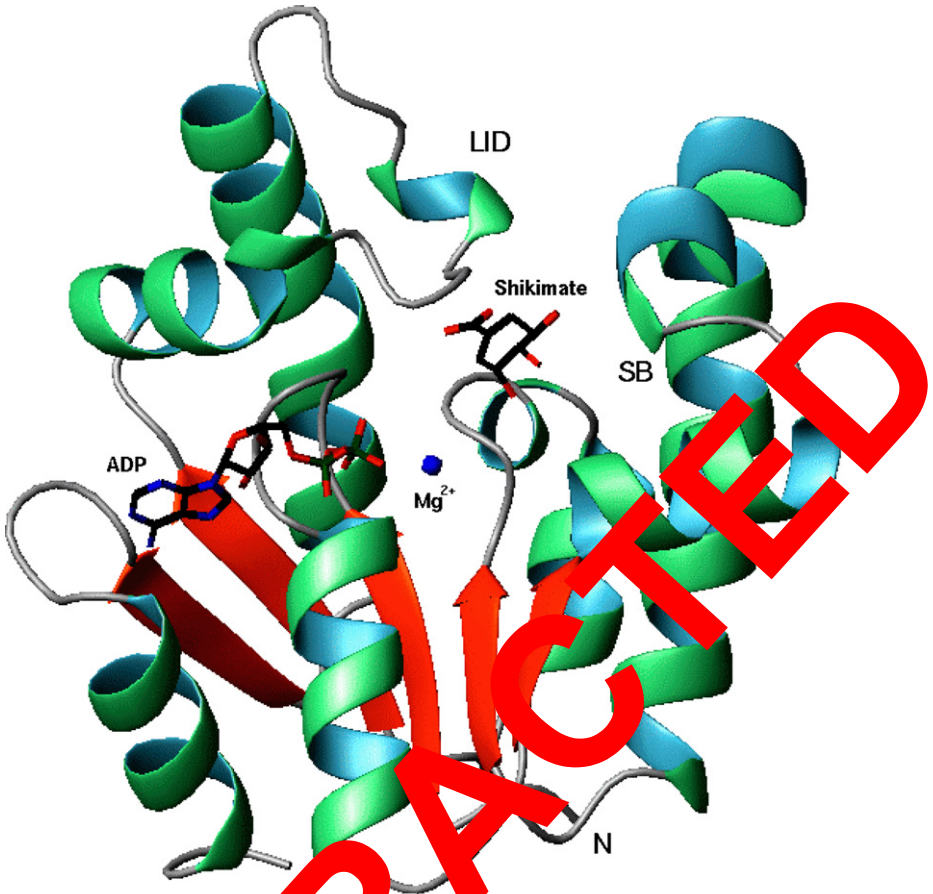

Fig. 1. MtSK complexed with Mg^{2+}, ADP, and shikimate (this work). LID (residues 112–124) and SB (residues 33–61) are responsible for large conformational changes during catalysis and are also shown. The figure was prepared with MOLMOL [35].

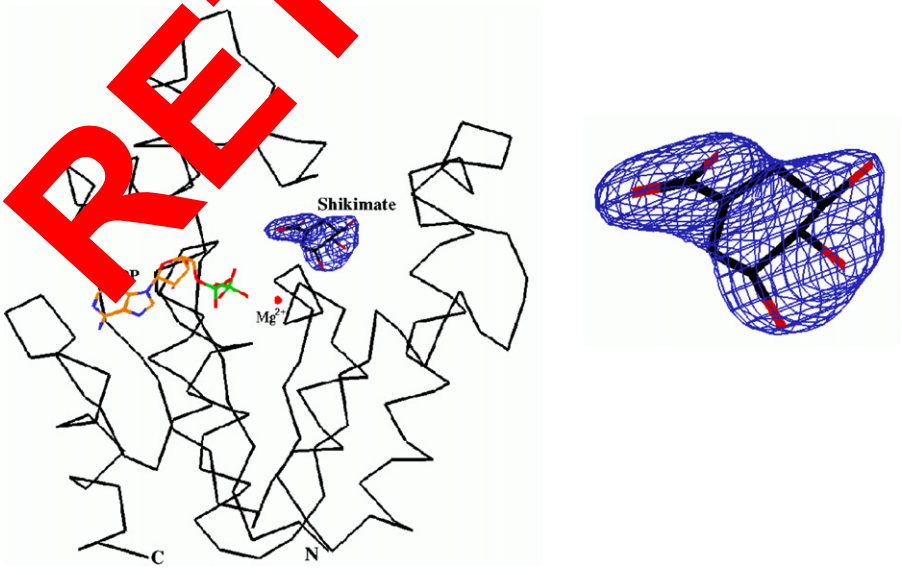

Fig. 2. The $F_{obs} - F_{calc}$ electron density contoured at 3.0σ showing the binding of shikimate. The figure was prepared with XtalView (McRee, 1999).

amide nitrogen of Ala82. Moreover, the NH1 atom of Arg58 forms a hydrogen bond with the O atom of Gly80. Therefore, the Glu61 residue plays an important role in positioning a shikimate molecule, even though it is not directly involved in substrate binding. Furthermore, the residue Glu61 is conserved in all SKs

RETRACTED

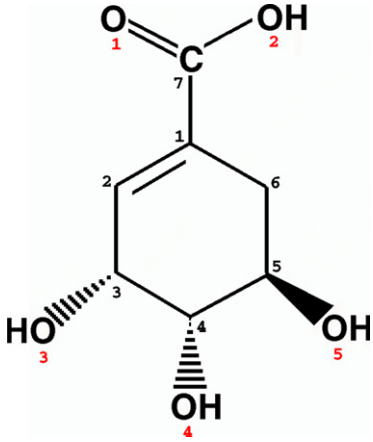

Fig. 3. Molecular structure of shikimate shows the carboxyl group and three hydroxyl groups. In black, numbering of atoms of carbons, and in red numbering of oxygen atoms. (For interpretation of the references to colors in this figure legend, the reader is referred to the web version of this paper.)

sequenced so far, which corroborates its role in anchoring Arg58 in the shikimate binding site. The Glu54 carboxylate group also appears to anchor the guanidinium group of Arg58 for interaction with shikimate carboxylate group, as suggested in the MtSK–MgADP structure [7]. However, Glu54 is not conserved, except for *aroK*-encoded shikimate kinases.

Conformational changes upon substrate binding

MtSK belongs to the family of nucleoside monophosphate (NMP) kinases, which are composed of three domains: CORE, LID, and NMP-binding domains. Kinases should undergo large movements during catalysis to shield their active center from water in order to avoid ATP hydrolysis [30]. The NMP and LID domains of NMP kinases have been shown to undergo large motions that are independent, in agreement with the observed random-bi-bi kinetics [15]. Ligand-induced changes in the secondary structure of EcSK have been detected by comparing circular dichroism spectra of free enzyme, EcSK–shikimate binary complex, and a ternary complex of EcSK, shikimate, and adenylyl imidodiphosphate, an ATP analog [8]. Alignment of C positions of MtSK–MgADP–shikimate dead-end ternary complex and MtSK–MgADP binary complex structures shows that the LID and SB domains undergo noticeable concerted movements toward each other (Fig. 4). The structural alignment included all residues and yielded rms deviation values of 0.5 and 0.7 Å for 1L4U and 1L4Y, respectively. The largest shift of the LID domain with an rms deviation of 1.33 Å is residues 112–124. The SB domain shift is somewhat smaller with a calculated rms deviation for residues 33–61 of 0.74 Å. The shikimate binding cavity is delineated mainly by residues from LID and SB domains, Walker B motif, and Arg136 from α7-helix. A close inspection of the residues involved in these movements shows that the side-chains of Val116, Pro118, and Leu119 from the LID domain, and Ile45, Ala46, Glu54, Phe57, and Arg58 from the SB domain shifted upon shikimate binding to MtSK–MgADP binary complex (Fig. 4). In MtSK with bound MgADP and shikimate, a cluster of hydrophobic contacts is formed between LID residues Val116, Pro118, and Leu119 and SB residues Ala46 and Phe49, which account for stabilization of partially closed shikimate-binding site cavity.

RETRACTED

Table 3
Direct and water-mediated hydrogen bonding of shikimate in MtSK

Shikimate	Atom	Distances (Å)	MtSK atom hydrogen bonded to water molecule	Distances (Å)
Hydroxyl groups				
O3	Gly79-N	3.10		
	Asp34-OD1	2.82		
	Asp34-OD2	2.57		
	Water320-O	2.46	Gly79-O	2.96
			Gly80-N	3.13
			Gly81-N	2.51
			Ala82-N	3.54
			Arg58-NH1	3.12
			Glu61-OE2	2.99
O4	Asp34-OD1	2.66		
	Asp34-OD2	2.85		
O5	n.o.[a]			
Carboxyl group				
O1	Gly81-N	3.22		
	Arg136-NH2	2.68		
O2	Arg58-NH2	2.67		
	Gly 81-N	3.49		
	Arg136-NH2	2.34		

All distances <3.6 Å are shown.
[a] Not observed.

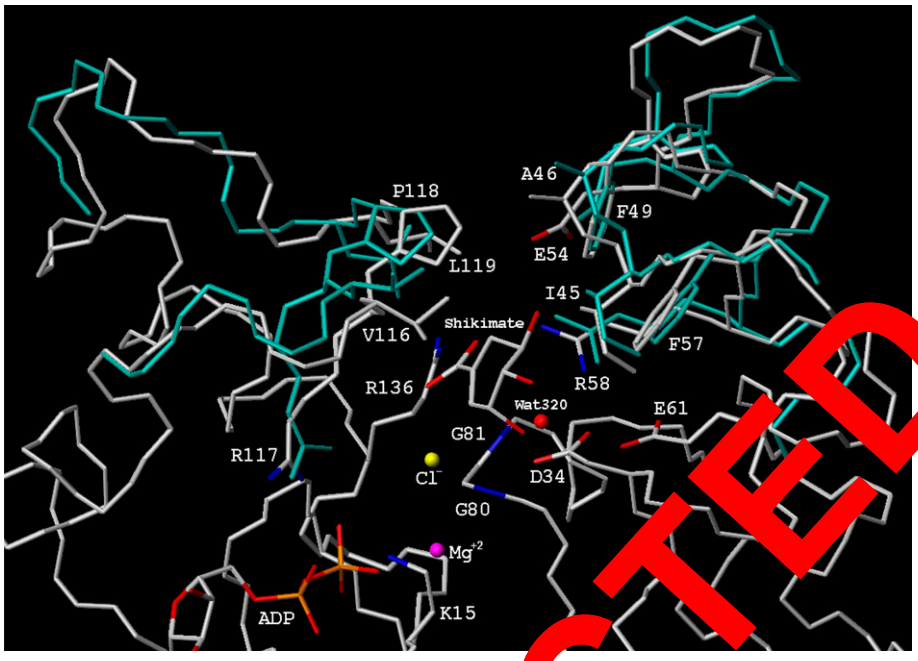

Fig. 4. Shikimate-binding of MtSK–MgADP–shikimate structure. The C^{α} atoms of MtSK–MgADP–shikimate and MtSK–MgADP (1L4U) [7] were superimposed and the C^{α} trace was colored by white and green, respectively. The side chains with larger shifts owing to shikimate binding are shown for both structures: Val116, Pro118, and Leu119 from LID domain; and Ile45, Ala46, Glu54, Phe57, and Arg58 from SB domain. For clarity only are shown residues from LID and SB domain of 1L4U (green). The side chains, shikimate, ADP, Mg^{2+}, and Cl^{-} ions, and the water molecule (Water320) of MtSK–MgADP–shikimate complex structure are colored by CPK (white for carbon, yellow for chlorine, red for oxygen, blue for nitrogen, orange for phosphorous, and purple for magnesium). (For interpretation of the references to colors in this figure legend, the reader is referred to the web version of this paper.)

RETRACTED

The conformational changes described above result in closure of MtSK-binding site as shown by the reduction of molecular surface areas for MtSK–shikimate–MgADP as compared to MtSK–MgADP. The ADP, Mg^{2+}, shikimate, Cl^{-} ions, and water molecules were removed prior to calculation. Calculated values are approximately 7246 $Å^2$ for MtSK complexed with MgADP (1L4U) and 6915 $Å^2$ for structure complexed with MgADP and shikimate. Thus, approximately 330 $Å^2$ of molecular surface is buried by shikimate binding. Since both MtSK–MgADP and MtSK–MgADP–shikimate have been crystallized in the same space group with similar values for cell parameters [31] (Table 1) and there are no crystal contacts of residues 114–124 from the LID domain and residues 33–61 from SB domain with symmetry-related MtSK molecules, the conformational changes observed may not merely be a reflection of the different crystal-packing arrangements.

The MtSK–MgADP–shikimate structure should represent a more partially, but not totally, closed structure, since total active site closure upon the dead-end ternary complex formation would result in locking the enzyme active site in an inactive form, in which shikimate substrate binding to MtSK enzyme prior to MgADP dissociation from its active site would result in an inactive abortive complex. Consistent with these structural results, measurements of EcSK intrinsic tryptophan fluorescence (Trp54) upon shikimate binding to either EcSK or EcSK–MgADP binary complex showed a modest synergism of binding between these substrates, since the dissociation constant value for shikimate ($K_d = 0.72$ mM) decreased to 0.3 mM in the presence of 1.5 mM ADP [32]. Measurements of quenching in protein fluorescence of the *aroL*-encoded EcSK upon nucleotide binding demonstrated that the dissociation constant values for ADP and ATP were 1.7 and 2.6 mM, respectively [9]. The K_m for ATP (620 μM) was found to be approximately four times lower than the dissociation constant in the absence of shikimate [9]. These results prompted the proposal that the conformational changes in the enzyme associated with binding of the first substrate lead to an increase in the affinity for the second substrate. However, even if it holds for EcSK, it does not appear to hold for MtSK since the apparent dissociation constant values for ATP (89 μM) and shikimate (44 μM) are similar to their K_m values, 83 μM for ATP and 41 μM for shikimate, considering a random-order bi-bi enzyme mechanism [7]. Moreover, no evidence for synergism between shikimate and ATP could be observed in substrate binding to EcSK in a chloride-free buffer system [33]. The K15M EcSK mutant has been crystallized in an open conformation proposed to presumably be equivalent to an apo-enzyme structure in which neither shikimate nor ADP (or ATP) would be bound [9]. This mutant was produced to evaluate the role of the conserved Lys15 of the Walker A

motif [9]. However, an unwanted point mutation in the LID domain (Pro115Leu) was detected during refinement of the model and extensive contacts between LID domains of neighboring EcSK enzymes were observed. It appears therefore unwarranted to consider the double K15M/P115L EcSK mutant a model for the apo-enzyme. The incomplete LID domain closure observed in the crystal structure presented here may suggest that the γ-phosphate of ATP plays a crucial role in the completion of the domain movement as has also been proposed by others [8]. The equilibrium constant value for the intramolecular hydrolysis of bound ATP to bound ADP and phosphate at enzyme active sites is considerably larger than the equilibrium constant for ATP hydrolysis in solution [34]. Accordingly, the loss of two water molecules (water5 and water6) described in "Interaction with ADP/Mg^{2+}" is consistent with exclusion of water molecules from the active site due to the partial closure of MtSK upon shikimate binding to minimize ATP hydrolysis.

Conclusions

Here we describe the residues involved in shikimate binding and conformational changes upon substrate binding to MtSK–MgADP complex, resulting in a partially closed structure. A complete active site closure could be achieved in a complex of MtSK with shikimate, Mg^{2+}, and the non-hydrolysable ATP analog adenosine 5′-(β,γ-methylene) triphosphate, AMP-PCP. A likely drawback of ATP-binding site based SK inhibitors would be their lack of specificity, owing to the common fold and similar ATP-binding site that many P-loop kinases share [20]. The availability of the *M. tuberculosis* shikimate kinase structure complexed with shikimate should allow the molecular design of specific SK inhibitors targeting either the shikimate- and ATP-binding sites or the shikimate binding site only. Moreover, the knowledge of functional factors that lead to active site closure could be used for designing inhibitors that force MtSK to a closed conformation that would be unable to catalyze the phosphoryl transfer to shikimate.

The atomic coordinates and structure factors (PDB access code 1WE2) have been deposited in the Protein Data Bank on May 22nd 2004, Research Collaboratory for Structural Bioinformatics, Rutgers University, New Brunswick, NJ (http://www.rcsb.org/).

Note added to the proof

An article describing the similar structure was published during the proofreading of this paper [36].

Acknowledgments

We acknowledge the expertise of Denise Cantarelli Machado for the expansion of cDNA library and Deise Potrich for the DNA sequencing. This work was supported by grants from FAPESP (SMOLBNet, Proc.01/07532-0 and 02/05347-4), CNPq, CAPES, and Instituto do Milênio (CNPq-MCT). W.F.A. (CNPq, 300851/98-7), D.S.S. (CNPq, 304051/76-9), M.S.P. (CNPq, 500079/90-0), and L.A.B. (CNPq, 520182/99-5) are researcher awardees from The National Research Council of Brasil – CNPq.

RETRACTED

References

[1] M.J. Whi... A.J. P...d, Reassessment of the relationship between ...K- and aro...oded shikimate kinase enzymes of *Esch...ia* ... J. Bacteriol. 177 (1995) 1627–1629.
[2] G. Millar, A. L...adon, M.G. Hunter, J.R Coggins, The cloning ...xpression o...e aroL gene from *Escherichia coli* K-12, Biochem. J. 237 (1986) 427–437.
R.C. De...eyter, J. Pittard, Purification and properties of ...hikimate ...ase II from *Escherichia coli* K-12, J. Bacteriol. 165 ...6) 33...533.
[4] B. L...J. Pittard, Aromatic amino acid biosynthesis: regulation of ...hikimate kinase in *Escherichia coli* K-12, J. Bacteriol. 138 (1979) ...–943.
[5] R.C. De Feyter, B.E. Davidson, J. Pittard, Nucleotide sequences of the transcription unit containing the aroL and aroM genes from *Escherichia coli* K-12, J. Bacteriol. 165 (1986) 233–239.
[6] D. Vinella, B. Gagny, D. Joseleau-Petit, R. D'Ardi, M. Cashel, Mecillinam resistance in *Escherichia coli* is conferred by loss of a second activity of the aroK protein, J. Bacteriol. 178 (1996) 3818–3828.
[7] Y. Gu, L. Reshetnikova, Y. Li, Y. Wu, H. Yan, S. Singh, X. Ji, Crystal structure of shikimate kinase from *Mycobacterium tuberculosis* reveals the dynamic role of the LID domain in catalysis, J. Mol. Biol. 319 (2002) 779–789.
[8] T. Krell, J.R. Coggins, A.J. Lapthorn, The three-dimensional structure of shikimate kinase, J. Mol. Biol. 278 (1998) 983–997.
[9] T. Krell, J. Maclean, D.J. Boam, A. Cooper, M. Resmini, K. Brocklehurst, et al., Biochemical and X-ray crystallographic studies on shikimate kinase: the important structural role of the P-loop lysine, Protein Sci. 10 (2001) 1137–1149.
[10] D. Dreusicke, A. Karplus, G.E. Schulz, Refined structure of porcine cytosolic adenylate kinase at 2.1 Å resolution, J. Mol. Biol. 199 (1988) 359–371.
[11] G.J. Schlauderer, G.E. Schulz, The structure of bovine mitochondrial adenylate kinase: comparison with isoenzymes in other compartments, Protein Sci. 5 (1996) 434–441.
[12] T. Stehle, G.E. Schulz, Three-dimensional structure of the complex of guanylate kinase from yeast with its substrate GMP, J. Mol. Biol. 211 (1990) 249–254.
[13] H.-J. Müller-Dieckmann, G.E. Schulz, The structure of uridylate kinase with its substrates, showing the transition state geometry, J. Mol. Biol. 236 (1994) 361–367.
[14] K. Wild, T. Bohner, A. Aubry, G. Folkers, G.E. Schulz, The three-dimensional structure of thymidine kinase from Herpes simplex virus type 1, FEBS Lett. 368 (1995) 289–292.
[15] C. Vonrhein, G.J. Schlauderer, G.E. Schulz, Movie of the structural changes during a catalytic cycle of nucleoside monophosphate kinases, Structure 3 (1995) 483–490.

[16] C.W. Müller, G.J. Schlauderer, J. Reinstein, G.E. Schulz, Adenylate kinase motions during catalysis: an energetic counterweight balancing substrate binding, Structure 4 (1996) 147–156.
[17] M. Gerstein, G.E. Schulz, C. Chothia, Domain closure in adenylate kinase: joints on either side of two helices close like neighbouring fingers, J. Mol. Biol. 229 (1993) 494–501.
[18] J.E. Walker, M. Saraste, M.J. Runswick, N.J. Gay, Distantly related sequences in the alpha- and beta-subunits of ATP synthase, myosin, kinases and other ATP-requiring enzymes and a common nucleotide binding fold, EMBO J. 1 (1982) 945–951.
[19] C.A. Smith, I. Rayment, Active site comparisons highlight structural similarities between myosin and other P-loop proteins, Biophys. J. 70 (1996) 1590–1602.
[20] D.D. Leipe, E.V. Koonin, L. Aravind, Evolution and classification of P-loop kinases and related proteins, J. Mol. Biol. 333 (2003) 781–815.
[21] I. Polikarpov, L.A. Perles, R.T. de Oliveira, G. Oliva, E.E. Castellano, R.C. Garratt, A. Craievich, Set-up and experimental parameters of the protein crystallography beam line at the Brazilian National Synchrotron Laboratory, J. Synchrotron Rad. 5 (1998) 72–76.
[22] A.G.W. Leslie, MOSFLM version 6.11 for processing image plate and CCD data, (1992).
[23] Collaborative Computational Project 4 The CCP4 suite: programs for protein crystallography, Acta Crystallogr. D50 (1994) 760–763.
[24] J. Navaza, AMoRe: an automated package for molecular replacement, Acta Crystallogr. A 50 (1994) 157–163.
[25] A.T. Brünger, X-PLOR Version 3.1: A System for Crystallography and NMR, Yale University Press, New Haven, 1992.
[26] D.E. McRee, XtalView/Xfit–A versatile program for manipulating atomic coordinates and electron density, J. Struct. Biol. 125 (1999) 156–165.
[27] R.A. Laskowski, M.W. MacArthur, D.K. Smith, D[illegible], E.G. Hutchinson, A.L. Morris, D. Naylor, D.S. [illegible]oss, J[illegible]. Thorton, PROCHECK v.3.0—Program to check the stereochemistry quality of Protein structures—Operating instructions, 1994.
[28] C.A. Hasemann, E.S. Istvan, K. Uyeda, J. Deisenhofer, The crystal structure of the bifunctional enzyme 6-phosphofructo-2-kinase/fructose-2,6-biphosphatase reveals distinct domain homologies, Structure 4 (1996) 1017–1029.
[29] M.J. Romanowski, S.K. Burley, Crystal structure of the *Escherichia coli* shikimate kinase I (AroK) that confers sensitivity to Mecillinam, Proteins: Struct Funct. Genet. 47 (2002) 558–562.
[30] W.P. Jencks, Binding energy, specificity and enzymatic catalysis: the circe effect, Adv. Enzymol. [illegible]19–410.
[31] Y. Gu, L. Reshetnikova, Y. Li, H. Ya[illegible], S.V. Singh, X. Ji, Crystallization and preliminary X-ray diffraction analysis of shikimate kinase from *Mycobacterium tuberculosis* in complex with MgADP, Acta Crystallogr. D5[illegible]) 1870–1871.
[32] C. Idziak, N.C. P[illegible]e, S.M. Kelly, T. Krell, D.J. Boam, A.J. Lapthorn, J.R. Cog[illegible]e interaction of shikimate kinase from *Erwinia chrysanthemi* [illegible] substrates, Biochem. Soc. Trans. 25 (1997) S62[illegible]
[33] E. Cer[illegible], M. Kelly, J.R. Coggins, A.J. Lapthorn, D.T. Clarke, N.C. Pr[illegible] Effects of salts on the function and conformational stability of shikimate kinase, Biochim. Biophys. Acta [illegible]8 (2003) 43–54.
[34] W.P. Jencks, Catalysis in Chemistry and Enzymology, Dover Publications, New York, USA, 1975.
[35] [illegible]. Koradi, M. Billeter, K. Wüthrich, MOLMOL: a program for display and analysis of macromolecular structures, J. Mol. Graph. [illegible]4 (1996) 51–55.
[36] [illegible]. Daliwal, C.E. Nichols, J. Ren, M. Lockyer, I. Charles, A.R. Hawkins, D.K. Stammers, Crystallographic studies of shikimate binding and induced conformational changes in *Mycobacterium tuberculosis* shikimate kinase, FEBS Lett. (2004).

RETRACTED